Optical and mechanical properties of plasma-beam-deposited amorphous hydrogenated carbon

Optical and mechanical properties of plasma-beam-deposited amorphous hydrogenated carbon

J. W. A. M. Gielen, P. R. M. Kleuskens, M. C. M. van de Sanden,[a)]
L. J. van Ijzendoorn, and D. C. Schram
Eindhoven University of Technology, Department of Applied Physics, P.O. Box 513, 5600 MB Eindhoven, The Netherlands

E. H. A. Dekempeneer and J. Meneve
Materials Department, Vlaamse Instelling voor Technologisch Onderzoek, Boeretang 200, B-2400 Mol, Belgium

(Received 3 June 1996; accepted for publication 25 July 1996)

Amorphous hydrogenated carbon films have been deposited on crystalline silicon and on glass from an expanding thermal plasma. Two deposition parameters have been varied: the electric current through the plasma source and the admixed acetylene flow. No energetic ion bombardment has been applied during deposition. *Ex situ* analysis of the films yields the infrared refractive index, hardness, Young's modulus, optical band gap, bonded hydrogen content, and the total hydrogen and mass density. The infrared refractive index describes the film properties independent of which plasma deposition parameter (arc current or acetylene flow) has been varied. The hardness, Young's modulus, sp^2/sp^3 ratio, and mass density increase with increasing refractive index. The optical band gap and hydrogen content of the films decrease with increasing refractive index. It is demonstrated that plasma-beam-deposited diamondlike *a*-C:H has similar properties as material deposited with conventional plasma-enhanced chemical-vapor-depositions techniques under energetic ion bombardment. © *1996 American Institute of Physics.* [S0021-8979(96)03621-3]

INTRODUCTION

Since the introduction of amorphous hydrogenated carbon (*a*-C:H) by Aisenberg and Chabot[1] in the early 1970s, the interest in this material has rapidly increased.[2] Responsible therefore are its very attractive properties: *a*-C:H is in general hard, chemically inert, electrically insulating, transparent to infrared light, and it exhibits low friction behavior. Moreover, the optical properties, such as the refractive index, can be tuned for the desired application.[3] Depending on the deposition conditions the material quality can vary from soft polymerlike *a*-C:H to hard diamondlike. The beneficial mechanical properties arise from sp^3 bonded carbon sites, while the optical and electronic properties are dependent on the sp^2 carbon sites.[4] Opposite to other carbon containing materials, such as, e.g., diamond, *a*-C:H can be deposited at low substrate temperature ($\leqslant$300 °C). The films find applications in the field of protective antireflection coatings on glass, e.g., in bar-code laser scanner devices, in file memory technology,[5] and in flat panel displays. Another major application is found as a wear-resistant, low-friction coating for mechanical systems. In general *a*-C:H films are produced via a plasma deposition technique[6] at a relatively low growth rate (0.1–1 nm/s).

For several years we have been depositing *a*-C:H from an expanding thermal plasma.[7–9] A major advantage of this technique compared to most commonly used plasma-enhanced chemical-vapor-deposition (PECVD) techniques[6] is the more efficient dissociation of the admixed precursors. This results in much higher growth rates, currently up to 75 nm/s for *a*-C:H material.

Recently, it has been shown that the quality of the films even improves with simultaneously increase of the growth rate.[9] These films have been deposited under variation of the plasma ionization degree and the admixed hydrocarbon flux. No additional substrate biasing has been applied and the energy of the ions therefore is determined by the self-bias which is only a few volts; thus, an energetic ion bombardment of the surface is not present. The object of this article is to show that the *a*-C:H film quality, using an expanding thermal plasma, is comparable to other PECVD techniques with respect to chemical structure and optical and mechanical properties.

DEPOSITION OF *a*-C:H

With the expanding thermal plasma technique, *a*-C:H films have been deposited on both crystalline silicon and glass substrates. A subatmospheric thermal arc plasma burns on argon. Acetylene is admixed in the arc exit, the nozzle. The formed plasma mixture expands into a vessel and is transported toward a substrate holder, which is water cooled. During deposition the substrate temperature is always below 100 °C, which is verified via infrared interferometry measurements.[10] No external substrate bias is applied. In Table I the plasma deposition settings are given. A detailed description of the setup is presented in Ref. 9.

Before deposition, the substrates (2.5×2.5 cm^2) are cleaned to obtain good adhesion of the film. The silicon ([100] oriented from Wacker-Chemitronic GMBH) and glass (Menzel-Gläser microscope slides) substrate cleaning is achieved by the following procedure: ultrasonic cleaning in diluted Decon Neutracon soap, rinsing with distilled water, ultrasonic cleaning in isopropyl alcohol, flushing with argon,

a)Electronic mail: m.c.m.v.d.sanden@phys.tue.nl

 0021-8979/96/80(10)/5986/10/$10.00

TABLE I. The deposition parameters for *a*-C:H.

Parameter	Value	Unit
Argon flow	100	sccs
Arc pressure	0.5	bar
Arc current	25–67	A
Arc power	1–5	kW
Acetylene flow	2–10	sccs
Vessel pressure	0.25	mbar
Distance from nozzle to substrate	65	cm
Substrate temperature at start	25	°C
Film thickness	2	μm

ultrasonic cleaning, and rinsing with distilled water, and finally flushing with argon.

The deposition procedure has a large influence on the final film quality. Before the substrates are introduced into the deposition setup, an argon/oxygen plasma (argon gas flow: 100 sccs; oxygen gas flow: 10 sccs; arc current: 48 A) is burned during 15 min. This is done to remove residual carbon from the chamber walls. The deposition procedure consists of the following steps: start the argon flow through the arc, ignite the plasma, start the injection of the acetylene precursor, and deposit a film for the required period, stop the acetylene addition, shut the plasma down, and finally stop the argon flow.

The addition of acetylene only when the plasma is burning turned out to be very important. When the acetylene is added before the plasma is ignited the adhesion of the film to the substrate is bad. One reason for this could be the fact that acetylene molecules easily chemisorb nondissociatively on a Si[100] surface at room temperature.[11] Another reason could be that interaction of low-energy argon ions is important before deposition starts. When the plasma is switched off before the acetylene addition is ceased, a film with a rather rough surface is the result. This is most probably due to direct deposition of acetylene on the growing film,[12] similar to the direct chemisorption on silicon. Additionally, an argon plasma after deposition can have a beneficial effect on the surface.

Two separate deposition sessions have been performed. In one session the arc current, which is a measure for the ionization degree of the primary gas flow, is varied from 25 to 67 A. This implies an arc power variation from 1 to 5 kW. The admixed acetylene flow is kept constant at 2 sccs. In the other session the acetylene flow is varied from 2 to 10 sccs at a constant arc current (48 A). The basic idea for these two plasma input parameter variations is that an increasing arc current results in more argon ions which leads to an enhanced ionization and dissociation of the hydrocarbon molecules and radicals; a variation of the acetylene flow affects the total flux of hydrocarbons toward the substrate.

The deposition time is chosen such that the deposited film thickness for all samples is around 1.5 μm. This is done in view of the *ex situ* hardness measurements with nanoindentation which require a minimal thickness of 1 μm. All films are found to adhere well to the substrate over more than 1 year after the film deposition.

FILM ANALYSIS

Analysis of the films has been performed with various *ex situ* diagnostics. Depth sensing nano-indention (NanoTest 500 instrument with a Berkovich indenter) has been used to obtain the hardness and Young's modulus.[13] To avoid substrate contributions the penetration depth has been limited to 300 nm. The indentation hysteresis curves have been analyzed applying the procedure proposed by Oliver and Pharr[14] after correction for the instrument compliance. No correction for the tip bluntness has been made, but during each measuring batch an uncoated silicon [111] substrate is indented under conditions similar to those of the *a*-C:H films. The results of each batch then are normalized on the literature hardness value of 12 GPa for silicon.[15] The hydrogen and carbon content of the films have been determined with elastic recoil detection analysis (ERDA) in combination with Rutherford backscattering (RBS).[16,17] The optical band gap has been obtained with transmission experiments in the range from 400 to 900 nm.[8] These are all standard techniques. Finally, the infrared transmission of the films has been measured with a Bruker IFS 66 Fourier transform infrared interferometer.[18,19]

The infrared transmission spectra for films on glass have been measured in the wave-number interval from 2000 to 5000 cm^{-1} with a resolution of 4 cm^{-1}. Below 2000 cm^{-1} glass exhibits a cutoff frequency and all incident light is absorbed. The spectra show clear interference patterns. These are caused by multiple reflection in the deposited films. Also absorption by carbon–hydrogen vibrations in the films is clearly visible around 3000 cm^{-1}. A typical example of a measured spectrum is given in Figure 1(a). In this spectrum also absorptions due to gas phase CO, CO_2 (around 2300 cm^{-1}), and water (around 3800 cm^{-1}) are present. These bonds are not present in the films themselves.

The measured spectra are fitted using an analytical expression given in Refs. 7 and 8. The background caused by multiple reflections in the *a*-C:H film has been fitted after removal of the features due to molecular bonds from the spectrum. The residual spectrum is then fully determined by the thickness and the refractive index which is assumed to be constant throughout the film. Subsequently, these two quantities are used as fit parameters. The fit is performed in the wave-number interval from 2400 to 3500 cm^{-1}. To check the validity of the assumption that the infrared refractive index is constant over the wave-number range, the spectrum is fitted for the whole measured wave-number interval (2000 to 5000 cm^{-1}). The maximum difference with the fit in the reduced wave-number interval is 7% vindicating the assumption made. The refractive index and thickness thus obtained are used as constants in the peak fit procedure.

The next step after the determination of the interference background is the deconvolution of the total absorption by C–H bonds into individual absorption peaks representing the specific stretching vibrations. In the literature it is often shown that the total absorption by C–H bonds is obtained by subtracting the fitted background spectrum from the total spectrum, i.e., including the molecular bonding regions. The absorption peaks then are fitted (see, e.g., Ref. 20); but, this procedure is analytically not correct and could lead to large

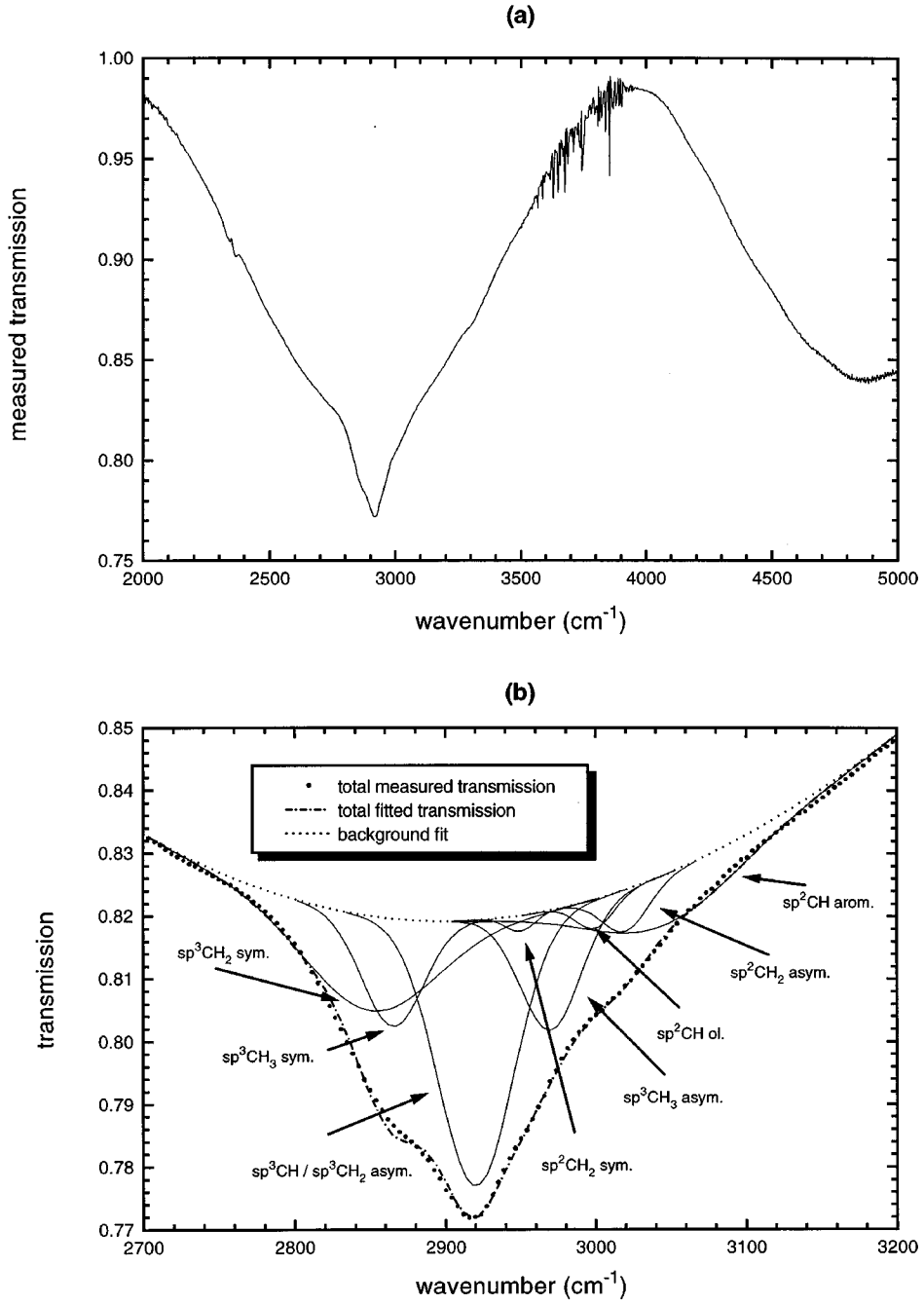

FIG. 1. A typical example of a (a) measured and (b) fitted infrared spectrum.

errors. However, the resulting fits are considered more or less reliable.

In our deconvolution procedure we apply the analytical description for the transmission already mentioned above. Each absorption peak is represented by a Gaussian function which has been proven to give good results[8,20] and is substituted into the transmission formula. The C–H vibrational absorption frequencies around 3000 cm^{-1} are given in Table II according to Dischler[21] and Dischler, Bubenzer, and Koidl.[22] Due to much overlap of the various peaks around 3000 cm^{-1} the deconvolution is rather complicated and some assumptions have to be made. One of them is the contribution of sp^3 CH_3 and sp^2 CH_2 bonds in the films. These bonds serve as end groups in the bond chain and result in soft polymerlike material. Dischler, Sah, and Koidl[23] have shown that in hard diamondlike *a*-C:H their presence is very small and sometimes even negligible. The peak fit, therefore, is performed stepwise. The sp^3 CH_3 and sp^2 CH_2 absorption peaks are left out in the first step. Furthermore, the maximum peak width is limited to 50 cm^{-1}.[21] With the remaining five peaks (see Table II) and the limited peak width, a fit is performed in the wave-number interval from 2700 to 3400 cm^{-1}. The peak positions are kept fixed, so the parameters varied are the peak area and the peak width. In all cases a rather good fit is found. Further improvement now is obtained by inserting either the sp^3 CH_3, the sp^2 CH_2, or both

TABLE II. The vibrational eigenfrequencies of C–H bonds.[a]

Bonding type	Stretching vibration [wave number (cm^{-1})]
sp^3 CH_2 symmetric	2850
sp^3 CH_3 symmetric	2865
sp^3 CH	2920
sp^3 CH_2 asymmetric	2920
sp^2 CH_2 olifinic, symmetric	2950
sp^3 CH_3 asymmetric	2970
sp^2 CH olifinic	3000
sp^2 CH_2 olifinic asymmetric	3020
sp^2 CH aromatic	3045
sp^1 CH	3300

[a]See Refs. 21 and 22.

vibrations in the fit function. For hard films, this only results in small contributions, as expected. As an example a fitted transmission spectrum from a polymerlike film is shown in Fig. 1(b). The sp^1 CH bond at 3300 cm^{-1} is also present in the spectra but is not shown.

RESULTS

In the literature many properties of *a*-C:H are given to characterize the material deposited. The hardness is known to be a very important mechanical property. For diamondlike *a*-C:H the hardness is found in the range from 10 to 20 GPa. Dekempeneer *et al.*[20] have presented a maximum value of about 14 GPa several years ago but currently they obtain hardnesses of 20 GPa for *a*-C:H deposited with an rf parallel-plate reactor. Robertson[4] and Pharr *et al.*[24] report a maximum value of 17 GPa. All these hardnesses are obtained at a substrate bias of about 200 V per deposited carbon particle. The optical band gap is found to be below 1.6 eV and the hydrogen density between 20 and 50% for diamondlike material.[4,20,25] Also the C–C bonding structure is known to be very important: sp^2 bonded carbon sites are responsible for the optical and electronic properties, while sp^3 bonded carbon sites determine the mechanical properties of the material.

In Fig. 2 the hardness of our films is given as a function of the infrared refractive index. It is found to vary from 3.5 GPa at low refractive index, indicating soft polymerlike material, to 12 GPa at high refractive index, indicating hard diamondlike material. The latter diamondlike quality is obtained without the use of an energetic ion bombardment of the surface as we do not apply any substrate bias. The plasma self-bias is also negligible; as the electron temperature is low ($\approx$0.2 eV) the self-bias is in the order of 1 V.[26] Furthermore, we have found that the highest hardness values are obtained when the residual argon-ion density, and thus ionization degree, in front of the growing film is minimal.[26,27] Modification of the film growth by an energetic ion bombardment thus seems not necessary to obtain diamondlike material. Concerning the hardness results it is evident that both the

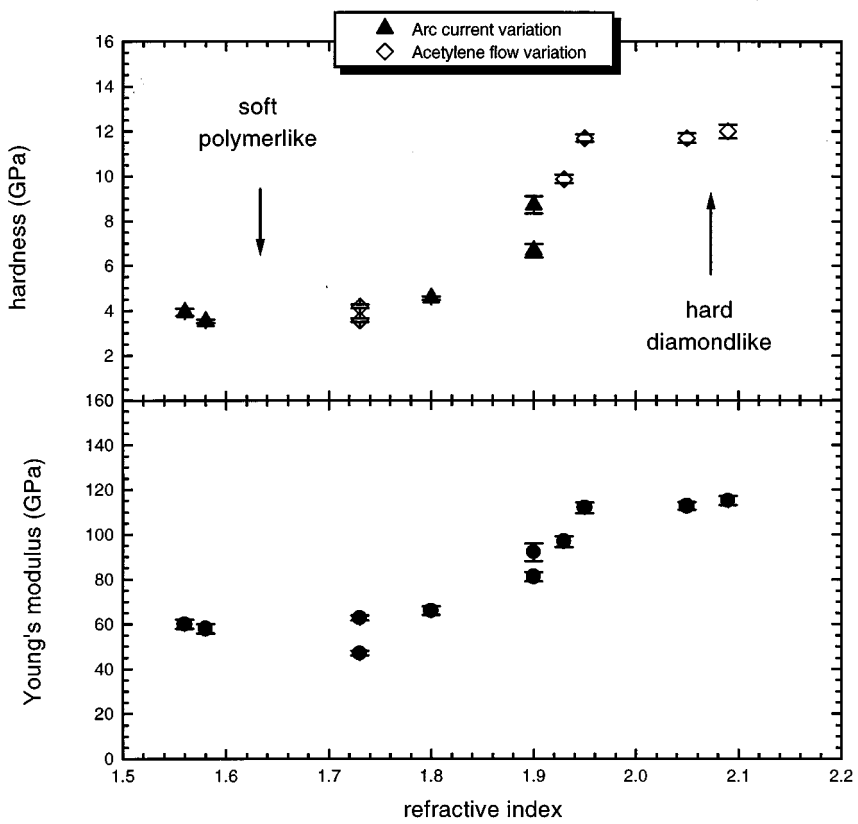

FIG. 2. The hardness and the Young's modulus vs the refractive index. The deposition parameters are given in Table I.

deposition series with arc current variation and acetylene flow variation align perfectly. Therefore, we conclude that the refractive index in the infrared region describes the film properties, which is confirmed throughout this article. This is in agreement with observations by, e.g., Cheshire *et al.*[28] and Donnelly *et al.*[29] All the following described properties are given as a function of the infrared refractive index which is an easy to determine parameter.

The Young's modulus, which describes the elastic behavior of the material, is given in Fig. 2. This quantity is found to increase for increasing refractive index which means that the resistance against elastic deformation increases. The ratio of the Young's modulus and the hardness varies from about 16, for polymerlike films, to nearly 10, for diamondlike *a*-C:H. This is in agreement with considerations by Bull[30] and Robertson *et al.*[4] They predict a ratio of about 10 or more for reliable hardness measurements which is based on calculations of the theoretical fracture strength of materials. Often in the literature much higher hardness values are given for diamondlike *a*-C:H but due to high elastic deformation these values are overestimated.

For *a*-C:H material it is known that a higher refractive index is accompanied by a decrease in the hydrogen content and an increase in the sp^2/sp^3 ratio.[4,25] Removing hydrogen and transformation of sp^3 bonds into sp^2 bonds allows more cross-linking and results in higher refractive indices. Further improvement of the material quality is obtained by the creation of more unhydrogenated sp^3 carbon. In theory both quantities can be obtained from infrared-absorption spectroscopy by fitting the C–H absorption peaks in the wave-number interval from 2800 to 3400 cm^{-1}; however, interpretation of the results has to be done with care. On one hand only bonded hydrogen is detected; the total hydrogen density therefore may be underestimated due to nonbonded hydrogen. On the other hand only carbon sites are detected which are connected to a hydrogen atom. In diamondlike material high cross-linking occurs between unhydrogenated sp^3 carbon sites which are invisible to infrared spectroscopy in the mentioned wave-number interval. The total sp^3 fraction thus might be underestimated and the sp^2/sp^3 ratio overestimated.[31,32] Before discussing the two quantities mentioned above the individual fitted absorption peaks are discussed qualitatively.

For all C–H bonding types present in our *a*-C:H material the fitted results are given in Fig. 3. They are shown as normalized peak areas defined by

$$\frac{sp^y\ \mathrm{CH}_x}{sp^y\ \mathrm{CH}_{x,\max}}, \tag{1}$$

with, for the sp^3 bonds, $y=3$, $x=1,2,3$; the sp^2 bonds: $y=2$, $x=1,2$, and the sp^1 bonds: $y=1$, $x=1$. The normalization is performed as only trends are to be discussed with varying refractive index. The normalization constants ($sp^y\ \mathrm{CH}_{x,\max}$) are given in Table III. All peak areas corresponding to sp^3 bonds decrease when going from polymerlike material to diamondlike *a*-C:H. For diamondlike material the sp^3 CH_3 bond even totally disappears. This is understood since this hybridization is an endgroup in the growing amorphous network which obstructs cross-linking and results in polymerlike material. Observations by Dischler[21] confirm this effect. The sp^3 CH bond is the dominant sp^3 bonding as it allows high cross-linking. Dischler[21] and Tanaka *et al.*[33] have found a similar behavior for diamondlike material. The observed net decrease in the sp^3 CH density is due to the fact that for diamondlike material more sp^3 bonds are formed between unhydrogenated carbon sites which are not detected by infrared spectroscopy.

With respect to the sp^2 hybridization (Fig. 3) the sp^2 CH_2 bonds, which decrease cross-linking, again are observed to disappear for diamondlike material. The sp^2 CH bond is the dominant sp^2 bond but the bonding structure changes from disordered olifinic sp^2 CH for polymerlike films to more ordered aromatic sp^2 CH for diamondlike material. This implies that in diamondlike *a*-C:H more aromatic clusters appear which is in agreement with the predictions of the cluster model by Robertson.[34]

More aromatic clusters in the films and a change of polymerlike to diamondlike material are expected to decrease the optical band gap.[34] In Fig. 4 the optical band gap is given as a function of the infrared refractive index. This band gap is determined from the spectroscopic measurements in the range from 400 to 900 nm applying Tauc's method.[35] For diamondlike material the band gap decreases to nearly 1 eV. This decrement is in agreement with the observed increase in the aromatic sp^2 bonds. From the cluster model of Robertson[4,34] a relation is obtained between the optical band-gap E_g (in eV) and the number of rings M per cluster,

$$E_g \approx \frac{6}{\sqrt{M}}. \tag{2}$$

Substitution of a band gap of 1 eV results in about 36 rings in one cluster.

If the absolute hydrogen content in the film is calculated from infrared spectroscopy several problems are encountered. In theory the absolute number of hydrogen atoms bonded to carbon N is calculated from[7,20]

$$N=\sum_i A_i \int \frac{\alpha_i(x)}{x}\,dx. \tag{3}$$

In this equation A_i is the proportionality constant and $\alpha_i(x)$ the absorption coefficient for each C–H vibration and x is the wave number. In the literature no consensus exists about the numerical value of the proportionality constant A_i. Dischler and co-workers[22] assumed about 10 years ago that all sp^y CH_x bonding types have the same proportionality constant. This assumption is adapted by most authors, e.g., Buuron *et al.*[7] and Fujimoto *et al.*[36] However, about 5 years ago Tanaka *et al.*[33] already argued that there should be different proportionality constants for each bonding type as is also the case for *a*-Si:H.[37] They measured and calculated the constants for the sp^3 CH_x bonds, using the relative intensity differences obtained by Fox and Martin[38] for the various bonds in gas phase measurements. Recently, Jacob and Unger[39] proposed a constant value for all different bonds which is only dependent on the hydrogen-to-carbon ratio in the deposited film; but, in the end they also conclude that it is more likely that for each bond itself a proportionality con-

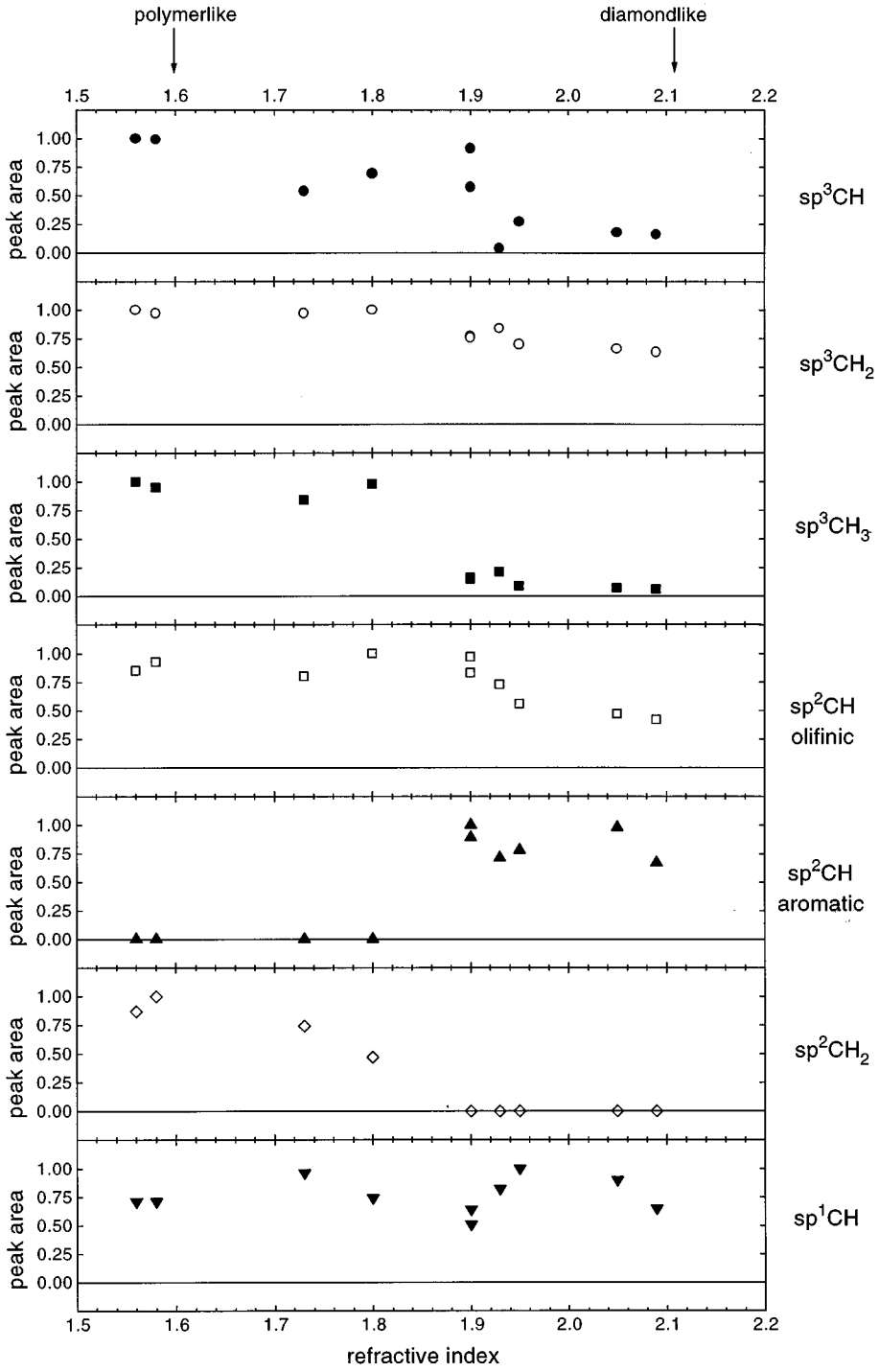

FIG. 3. The normalized fitted peak area for sp^y CH_x bonds vs refractive index. The deposition parameters are given in Table I.

stant exists. A solution for the depicted problem is not yet available and still assumptions have to be made. Another problem which is encountered is that infrared spectroscopy, as already mentioned, only detects bonded hydrogen. The total hydrogen density thus might be underestimated.

Assuming a constant proportionality constant for all (C–H) bonds the relative density of sp^1, sp^2, and sp^3 hybridized C–H bonds has been calculated from the fitted peak areas. Several C–H bonds exhibit a symmetric and asymmetric vibration (see Table II). Only one vibration is used for

TABLE III. The normalization constants for the fitted peak areas.

Bonding type	Normalization constant
sp^3 CH	0.56
sp^3 CH_2	0.95
sp^3 CH_3	0.36
sp^2 CH olifinic	0.48
sp^2 CH aromatic	0.26
sp^2 CH_2	0.21
sp^1 CH	0.07

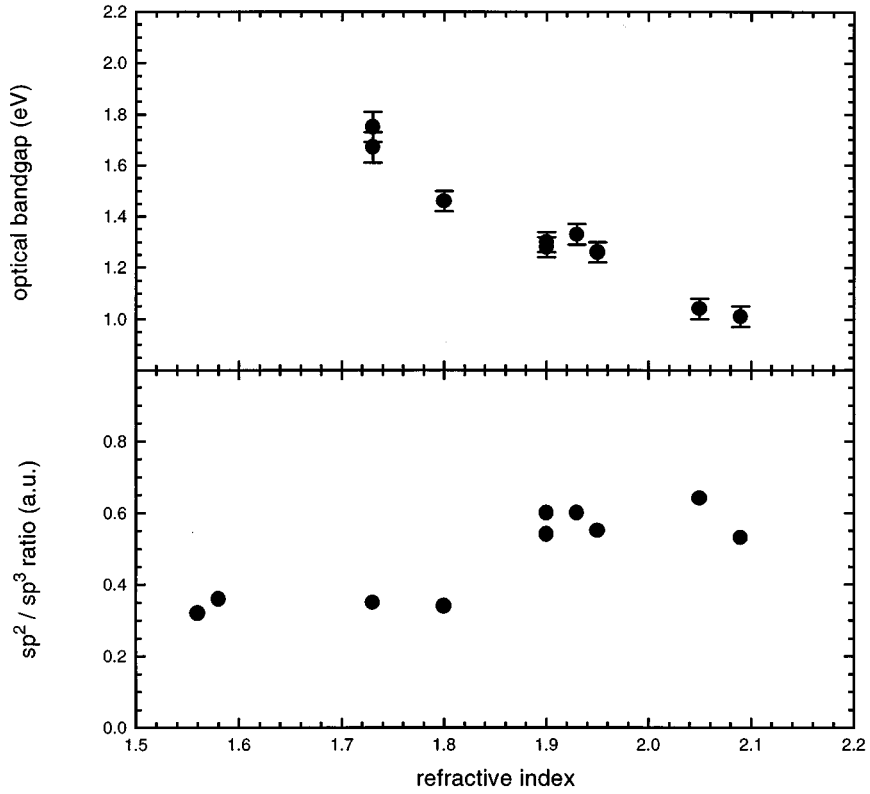

FIG. 4. The optical band gap and sp^2/sp^3 ratio vs the refractive index. The deposition parameters are given in Table I.

each bond: the asymmetric one for the sp^3 bonds and the symmetric one for the sp^2 bonds. For harder material the relative sp^3 density decreases, due to more cross-linking between unhydrogenerated C–C bonds; in an absolute sense there is also a decrease. The relative sp^2 density is observed to increase. This, however, is no absolute increase. It is only due to a decrease of the sp^3 density. For harder material only a transformation from olifinic to aromatic bonded sp^2 occurs. The contribution of sp^1 bonds is very small ($\leqslant 5\%$), which is not surprising as this bonding type is also an end group in a chain. The sp^1 contribution is rather independent of the refractive index as also can be seen in Fig. 3. The appearance of a small amount of sp^1 in the films suggests that the substrate temperature has never exceeded 100 °C during deposition.[21]

The sp^2/sp^3 ratio has been calculated under the assumption of one fixed proportionality constant for all bonding types. The result is presented in Fig. 4. The sp^2/sp^3 ratio is found to increase with refractive index increment. This increase is mainly caused by the decrease of sp^3 bonded carbon sites, due to more unhydrogenated C–C cross-linking. The observed behavior is in agreement with the determined decrease in the optical band gap. The appearance of relatively more aromatic sp^2 bonded carbon than sp^3 bonded carbon results in a lower band gap and more absorption at lower photon energies.

The determination of the absolute hydrogen density from infrared spectroscopy is strongly dependent on the values for the used proportionality constants. As earlier mentioned, no exact values are known from literature. In order to find reasonable proportionality constant values we have applied a second independent diagnostic to determine the hydrogen density in the films: ERDA/RBS. Only for the highest refractive indices is the hydrogen content measured with this technique. The result is given in Fig. 5: The density decreases from about 5×10^{22} to 4×10^{22} cm^{-3}. This is equivalent with a decrease from 45 to 35 at. % hydrogen which is in agreement with observations by, e.g., Dekempeneer *et al.*[20]

Calculation of the proportionality constants is performed by relating the ERDA/RBS to the infrared measurements. It is assumed that no unbonded hydrogen is present in the films as we have no energetic ion bombardment which releases hydrogen via subsurface rearrangement of the growing film. Two different relations are adapted between the proportionality constants of the various bondings. The proportionality constants then are determined via a least-squares fit of the ERDA/RBS data and the infrared data which are related via Eq. (3).

In the first case we follow the procedure of Tanaka *et al.*[33] The proportionality constants are dependent on the specific bonding type. Therefore, the results obtained for hydrocarbon gasses by Fox and Martin[38] are used: The relative absorption intensities between the various bonds are fixed and given by

$$sp^3\mathrm{CH} : sp^3\mathrm{CH_2} : sp^2\mathrm{CH} : sp^1\ \mathrm{CH} = 1:10:3.4:3.4. \qquad (4)$$

The value for the sp^1CH bond, which is not given by Fox and Martin, is assumed to be the same as for sp^2 CH. Be-

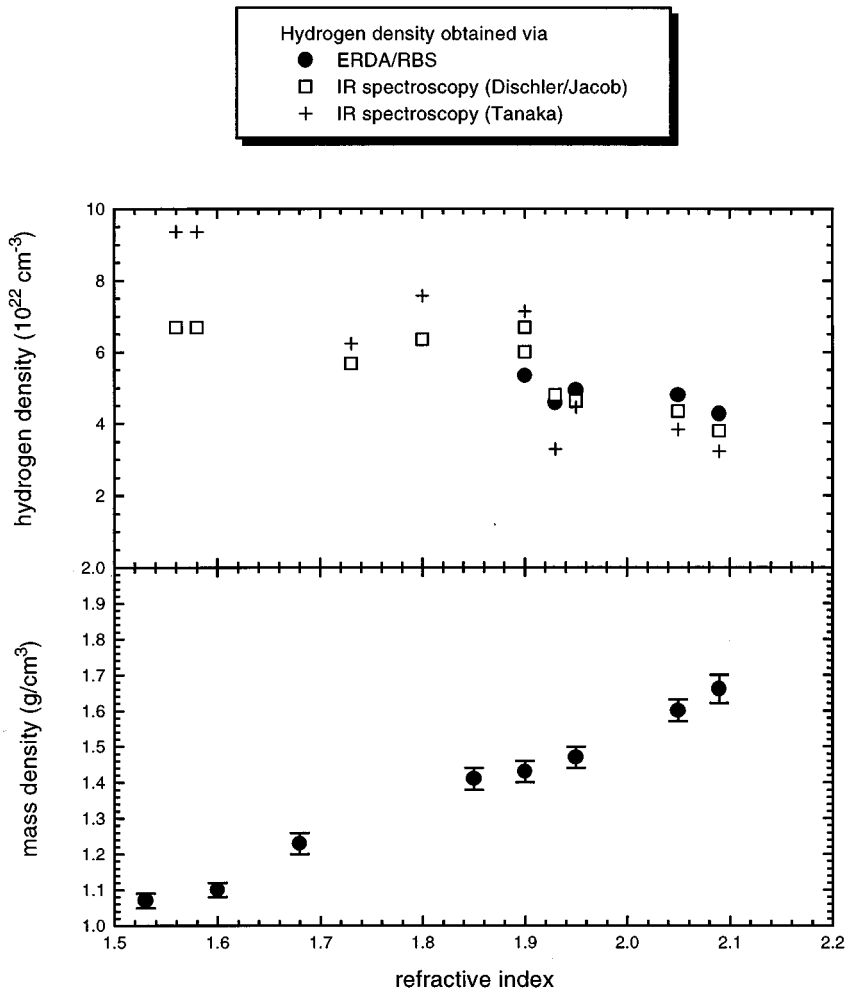

FIG. 5. The hydrogen density from infrared-absorption spectroscopy and ERDA/RBS, and the mass density vs the refractive index. The deposition parameters are given in Table I.

cause the contribution of the sp^1 bond in the material is small, as already mentioned, this assumption is allowed. For the sp^3 CH bond this results in a proportionality constant of 9.5×10^{21} cm^{-2}. The other proportionality constants then are calculated via Eq. (4). The hydrogen density obtained via the infrared measurements and the appropriate proportionality constants is given in Fig. 5. The hydrogen density decreases from about 9×10^{22} to 3×10^{22} cm^{-3} and is in rather good agreement with the ERDA/RBS values.

In the second case one proportionality constant is assumed for all bonding types as, e.g., is assumed by Dischler and co-workers[22] and Jacob and Möller.[31] This results in an overall value of 2.7×10^{21} cm^{-2} for all bonding types. The calculated hydrogen density (Fig. 5) then decreases from about 7×10^{22} to 4×10^{22} cm^{-3}. In this case better agreement is obtained with the ERDA/RBS measurements for higher refractive indices.

Comparison of the obtained proportionality constants with the literature data reveals that our values are higher for both situations. Tanaka *et al.*[33] find 3.85×10^{21} cm^{-2} for the sp^3 CH bond. We find 9.5×10^{21} cm^{-2}. Jacob and Möller[31] as an example for a constant proportionality constant for all bondings, report a maximum value below 10^{21} cm^{-2}. This value is adapted by most authors. We find 2.7×10^{21} cm^{-2}. These lower constants are most probably due to the fact that they use the total integrated absorption peak, including both symmetric and asymmetric vibrations (Table II). This implies a double counting of hydrogen to carbon bonds and results in lower constants. In our opinion the proportionality constants are dependent on the specific bonding type. The sp^3 CH constant then should be between 2 and 10×10^{21} cm^{-2}.

The mass density is also calculated from ERDA/RBS in combination with an independent determination of the film thickness via infrared spectroscopy. The result is presented in Fig. 5. The density increases from about 1.0 to 1.7 g/cm^3 with increasing refractive index. This is in agreement with earlier results.[4,25] It once more confirms the observed hardness increment.

The film properties of our *a*-C:H material are summarized in Table IV. The best films are those with the highest hardness (about 12 GPa); they have infrared refractive indices between 1.95 and 2.09. In this table also the diamondlike properties of *a*-C:H films deposited with other PECVD techniques[4,20,25,40–42] are given. As is obvious the highest obtained quality of the plasma beam deposited *a*-C:H is of a

TABLE IV. Overview of the film properties of plasma-beam-deposited diamondlike a-C:H and films deposited with other PECVD techniques.[a]

Film property	Plasma beam deposition	PECVD
Hardness (GPa)	12	10–20
Optical band gap (eV)	1.0–1.3	1.0–1.6
Mass density (g/cm^3)	1.5–1.7	1.4–1.9
Hydrogen content (at. %)	35–45	20–50
Refractive index: visible	≈2.1	1.8–2.5
Infrared	1.95–2.09	1.6–2.3

[a]See Refs. 4, 20, 25, and 40–42.

diamondlike nature. This is surprising as, opposite to the a-C:H material obtained via other PECVD methods, no substrate biasing has been applied. Only variation of the ionization degree of the plasma emanating from the cascaded arc source and the admixed acetylene flow has been performed without applying an energetic ion bombardment of the growing film. This is contrary to the general expectation that energetic ions with energies between 50 and 200 eV are needed for good film quality.[25,40,43–46] These ions are supposed to be necessary for subsurface reorganization of the growing film.[47] During the plasma beam deposition of diamondlike a-C.H the subsurface reorganization does not seem essential. This suggests that the plasma composition and surface chemistry might play a decisive role for the quality determination; however, a full explanation is not yet available.

CONCLUSIONS

Amorphous hydrogenated carbon films have been deposited on crystalline silicon and on glass, from an expanding thermal plasma. The deposition parameters varied are the electric current through the arc and the admixed acetylene flow. No energetic ion bombardment is applied to the substrate. The films have been analyzed *ex situ* yielding the infrared refractive index, hardness, Young's modulus, optical band gap, bonded hydrogen structure and density, total hydrogen density, and the mass density.

The film properties depend on the infrared refractive index independent of which deposition parameter is varied. The film properties change from polymerlike at low refractive index to diamondlike at high refractive index. The hardness, Young's modulus, sp^2/sp^3 ratio, and mass density increase at increasing refractive index; the hydrogen density and optical band gap then decrease.

Comparison with diamondlike a-C:H deposited from other PECVD techniques under energetic ion bombardment reveals that plasma-beam-deposited diamondlike a-C:H exhibits similar material quality.

ACKNOWLEDGMENTS

The skilful technical assistance of M. J. F. van de Sande, A. B. M. Hüsken, and H. M. M. de Jong is greatly acknowledged. The Foundation of Fundamental Research on Matter (FOM) and the Royal Netherlands Academy for Arts and Sciences (KNAW) are thanked for their financial support. The European Community is acknowledged for supporting this work via the Human Capital and Mobility Programme (networks), Contract No. CHRX-CT94-0575.

[1] S. Aisenberg and R. Chabot, J. Appl. Phys. **42**, 2953 (1971).
[2] J. C. Angus and Y. Wang, in *Diamond and Diamond-like Films and Coatings*, edited by R. E. Clausing, L. L. Horton, J. C. Angus, and P. Koidl, NATO ASI Series B, Vol. 266 (Plenum, New York, 1991), p. 173.
[3] J. C. Angus, P. Koidl, and S. Domitz, in *Plasma Deposited Thin Films*, edited by J. Mort and F. Jansen (CRC, Boca Raton, FL, 1986), p. 89.
[4] J. Robertson, Surf. Coat. Technol. **50**, 185 (1992).
[5] S. Miyake and R. Kaneko, Thin Solid Films **212**, 256 (1993).
[6] Y. Catherine, in *Diamond and Diamond-like Films and Coatings*, edited by R. E. Clausing, L. L. Horton, J. C. Angus, and P. Koidl, NATO ASI, Series B, Vol. 266 (Plenum, New York, 1991), p. 193.
[7] A. J. M. Buuron, M. C. M. van de Sanden, W. J. van Ooij, R. M. A. Driessens, and D. C. Schram, J. Appl. Phys. **78**, 528 (1995).
[8] J. W. A. M. Gielen, M. C. M. van de Sanden, and D. C. Schram, Thin Solid Films **271**, 56 (1995).
[9] J. W. A. M. Gielen, M. C. M. van de Sanden, P. R. M. Kleuskens, and D. C. Schram, Plasma Sources Sci. Technol. **5**, 492 (1996).
[10] E. S. Aydil, J. A. Gregus, and R. A. Gottscho, Rev. Sci. Instrum. **64**, 3572 (1993).
[11] M. Nishijima, J. Yoshinobu, H. Tsuda, and M. Onchi, Surf. Sci. **192**, 383 (1987).
[12] S. A. Miller, *Acetylene, Its Properties, Manufacture and Uses* (Ernest Benn, London, 1965).
[13] J. L. Loubet, J. M. Georges, and G. Meile, in *Vickers Indentation Curves of Elastoplastic Materials, Microindentation Techniques in Materials Science and Engineering*, edited by P. J. Blau and B. R. Lawn, ASTM Spec. Techn. Publ., No. 889 (ASTM, Philadelphia, PA, 1986), p. 72.
[14] W. C. Oliver and G. M. Pharr, J. Mater. Res. **7**, 1564 (1992).
[15] E. R. Weppelmann, J. S. Field, and M. V. Swain, J. Mater. Res. **8**, 830 (1993).
[16] L. J. Van IJzendoorn, Anal. Chem. Act. **297**, 55 (1994).
[17] L. C. Feldman and J. W. Mayer, *Fundamentals of Surface and Thin Film Analysis* (North-Holland, New York, 1986).
[18] J. T. Houghton and S. D. Smith, *Infrared Physics* (Oxford University Press, Oxford, 1966).
[19] N. L. Alpert, W. E. Keiser, and H. A. Szymanski, *IR Theory and Practice of Infrared Spectroscopy* (Plenum, New York, 1973).
[20] E. H. A. Dekempeneer, R. Jacobs, J. Smeets, J. Meneve, L. Eersels, B. Blanpain, J. Roos, and D. J. Oostra, Thin Solid Films **217**, 56 (1992).
[21] B. Dischler, E-MRS Meeting **17**, 189 (1987).
[22] B. Dischler, A. Bubenzer, and P. Koidl, Solid State Commun. **48**, 105 (1983).
[23] B. Dischler, R. E. Sah, and P. Koidl, in *Proceedings of ISPC-11*, edited by C. J. Timmermans (Eindhoven, The Netherlands, 1985), p. 45.
[24] G. M. Pharr, D. L. Callahan, S. D. McAdams, T. Y. Tsui, S. Anders, A. Anders, J. W. Ager III, I. G. Brown, C. S. Bhatia, S. R. P. Silva, and J. Robertson, Appl. Phys. Lett. **68**, 779 (1996).
[25] N. Fourches and G. Turban, Thin Solid Films **240**, 28 (1994).
[26] J. W. A. M. Gielen, M. C. M. van de Sanden, W. M. M. Kessels, and D. C. Schram, in *Thin Films: Stresses and Mechanical Properties VI*, Mater. Res. Soc. Proc., edited by W. W. Gerberich, H. Gao, and J.-E. Sundgren (MRS, Pittsburgh, PA, in press).
[27] J. W. A. M. Gielen, M. C. M. van de Sanden, and D. C. Schram, Appl. Phys. Lett. **69**, 152 (1996).
[28] R. C. Cheshire, W. G. Graham, T. Morrow, V. Komas, H. F. Döbele, K. Donnelly, D. P. Dowling, and T. P. O'Brien, Appl. Phys. Lett. **66**, 3152 (1995).
[29] K. Donnelly, D. P. Dowling, E. Davitt, T. P. O'Brien, and T. C. Kelly, in *Proceedings, Advances in Materials Processing Technologies '93 Dublin*, edited by M. S. J. Hashmi (1993), p. 769.
[30] S. J. Bull, Diam. Relat. Mater. **4**, 827 (1995).
[31] W. Jacob and W. Möller, Appl. Phys. Lett. **63**, 1771 (1993).
[32] C. De Martinu, F. Demichelis, and A. Tagliaferro, Diam. Relat. Mater. **4**, 1210 (1995).
[33] M. Tanaka, Y. Iwata, F. Fujimoto, K. Komaki, K. Kobayashi, H. Yamashita, and M. Haba, Nucl. Instrum. Methods Phys. Res. B **45**, 223 (1990).
[34] J. Robertson, Diam. Relat. Mater. **4**, 297 (1995).

[35] J. Tauc, in *Optical Properties of Solids*, edited by F. Abelès (North-Holland, Amsterdam, 1972).
[36] F. Fujimoto, A. Ootuka, K. Komaki, Y. Iwata, I. Yamane, H. Yamashita, Y. Hashimoto, Y. Tawada, K. Nishimura, H. Okamoto, and Y. Hamakawa, Jpn. J. Phys. **23**, 810 (1984).
[37] A. A. Langford, M. L. Fleet, B. P. Nelson, W. A. Langford, and N. Maley, Phys. Rev. B **45**, 13 367 (1992).
[38] J. Fox and A. Martin, Proc. R. Soc. London, Ser. A **175**, 208 (1940).
[39] W. Jacob and M. Unger, Appl. Phys. Lett. **68**, 475 (1996).
[40] P. Koidl, C. Wild, R. Locher, and R. E. Sah in *Diamond and Diamond-like Films and Coatings*, edited by R. E. Clausing, L. L. Horton, J. C. Angus, and P. Koidl, NATO ASI Series B, Vol. 266 (Plenum, New York, 1991), p. 243.
[41] J. Robertson, in *Diamond and Diamond-like Films and Coatings*, edited by R. E. Clausing, L. L. Horton, J. C. Angus, and P. Koidl, NATO ASI Series B, Vol. 266 (Plenum, New York, 1991), p. 331.
[42] O. Stenzel, R. Petrich, and M. Vogel, Opt. Mater. **2**, 125 (1993).
[43] P. Reinke, W. Jacob, and W. Möller, J. Appl. Phys. **74**, 1354 (1993).
[44] A. von Keudell, W. Jacob, and W. Fukarek, Appl. Phys. Lett. **66**, 1322 (1995).
[45] S. Xu, M. Mundhausen, J. Ristein, B. Yan, and L. Ley, J. Non-Cryst. Solids **164–166**, 1127 (1993).
[46] L. Martinu, A. Raveh, A. Dominique, L. Bertrand, J. E. Klemberg-Sapieha, S. C. Gujrathi, and M. R. Wertheimer, Thin Solid Films **208**, 42 (1992).
[47] A. von Keudell, in *Film Synthesis and Growth Using Energetic Beams*, edited by H. A. Atwater, J. T. Dickinson, D. H. Lowndes, and A. Polman, Mater. Res. Soc. Proc., Vol. 388 (MRS, Pittsburgh, PA, 1995), p. 355.